Signal-to-noise limitations in white light holography

Erez Ribak, Claude Roddier, Francois Roddier, and James B. Breckinridge

A simple derivation is given for the signal-to-noise ratio (SNR) in images reconstructed from incoherent holograms. Dependence is shown to be on the hologram SNR, object complexity, and the number of pixels in the detector. Reconstruction of involved objects becomes possible with high dynamic range detectors such as charge-coupled devices. We have produced such white light holograms by means of a rotational shear interferometer combined with a chromatic corrector. A digital inverse transform recreated the object.

I. Introduction

Incoherent optical Fourier transforms have an advantage over coherent transforms in that they can be performed on natural white-light scenes as well as on simple input devices [cathode ray tubes (CRTs), image intensifiers]. They are also less sensitive to coherent noise and to system vibrations. In this paper we investigate the noise characteristics of such transforms.

An incoherent optical Fourier transform is obtained when each point of an incoherent object produces a distinct sinusoidal fringe pattern. The incoherent addition of all the fringe patterns produces the object Fourier transform. This is the case when an interferometer gives two images of an incoherent object, one being rotated with respect to the other.[1-14] Let $o(\mathbf{x})$ be the irradiance distribution in the incoherent object. Without loss of generality we shall assume that the object is at infinity so that $\mathbf{x}$ is a pair of angular coordinates expressed in radians. The irradiance distribution $I(\mathbf{u})$ in the hologram can be written in a general way:

$$I(\mathbf{u}) = O(0) + \mathrm{Re}O(kR\mathbf{u}/\lambda), \tag{1}$$

where $\mathrm{O}(\cdot)$ is the Fourier transform of $o(\cdot)$, k is a magnification factor, R is a rotation operator, and λ is the wavelength. The Fourier transform $i(\cdot)$ of the irradiance distribution in the hologram gives

$$(k/\lambda)^2 i(kR^{-1}\mathbf{x}/\lambda) = O(0)\delta(\mathbf{x}) + \tfrac{1}{2}[o(\mathbf{x}) + 0(-\mathbf{x})], \tag{2}$$

where R^{-1} is the inverse rotation and $\delta(\mathbf{x})$ is a Dirac distribution. Equation (2) shows that the object can be recovered from the hologram as long as it does not overlap with its mirror image with respect to the interferometer axis. Another limitation is that the transform has to be either narrowband or chromatically corrected to utilize the polychromatic nature of real-life objects [and increase the signal-to-noise ratio (SNR) of the transform]. Many efforts have been conducted[15-18] toward a solution to this limitation. For involved objects, the dc component (which may also include scattered light) creates a demand for a high dynamic range detector.

Incoherent holography might be called as well Fourier transform imaging, since it is formally similar to Fourier transform spectroscopy,[19] time being here replaced with a 2-D space variable. Theoretical analyses of Fourier transform spectroscopy directly apply to Fourier transform imaging.

II. Signal-to-Noise Ratio in the Reconstructed Image

The SNR for the reconstructed image has been discussed by Lowenthal *et al.*[20] Here we adapt a derivation due to Mertz[1] for the SNR in Fourier transform spectroscopy. The noise n_O in the reconstructed image is a scaled version of the Fourier transform of the noise N_I in the hologram. According to Eq. (2), the Parseval theorem gives

$$\int |N_I(\mathbf{u})|^2 d\mathbf{u} = (\lambda/k)^2 \int |n_O(\mathbf{x})|^2 d\mathbf{x}, \tag{3}$$

which can be written

$$\overline{N_I^2} A = (\lambda/k)^2 \overline{n_O^2} a', \tag{4}$$

where A is the hologram area and a' is the mean area over which noise extends in the plane of the reconstructed image. $\overline{N_I}$ and $\overline{n_O}$ are the average rms noises in the hologram and the reconstructed image, respectively. We assume here that the reconstructed image is obtained from Eq. (2), although taking the real part of it would reduce the noise by a factor of $\sqrt{2}$.

Let a be the area over which the reconstructed image extends. The average signal in the image is

$$\bar{o} = \frac{1}{a}\int o(\mathbf{x})d\mathbf{x} = \frac{O(0)}{a} = \frac{\bar{I}}{a}, \tag{5}$$

where $\bar{I}$ is the average illumination in the hologram [Eq. (1)]. We estimate the SNR for the reconstructed image as

Erez Ribak and J. B. Breckinridge are with California Institute of Technology, Jet Propulsion Laboratory, Pasadena, California 91109; the other authors are with National Optical Astronomy Observatories, ADP Division, P.O. Box 26732, Tucson, Arizona 85726.

Received 4 July 1987.
0003-6935/88/061183-04$02.00/0.

$$\mathrm{SNR}_{\mathrm{rec}} = \frac{\bar{o}}{\overline{n_O}}. \tag{6}$$

Putting Eqs. (4) and (5) into Eq. (6) yields

$$\mathrm{SNR}_{\mathrm{rec}} = \frac{\sqrt{a'}}{a\sqrt{A}} \frac{\lambda}{k} \frac{\bar{I}}{\overline{N_I}}. \tag{7}$$

Since the smallest resolved area in the image plane is $(\lambda/k)^2 A^{-1}$, one can introduce in Eq. (7) the number $M = (k/\lambda)^2 aA$ of resolved pixels in the image yielding

$$\mathrm{SNR}_{\mathrm{rec}} = \frac{\sqrt{a'}}{\sqrt{A}} \frac{1}{\sqrt{M}} \frac{\bar{I}}{\overline{N_I}} = \frac{\sqrt{a'}}{\sqrt{a}} \frac{1}{\sqrt{M}} \mathrm{SNR}_{\mathrm{hol}}, \tag{8}$$

where $\mathrm{SNR}_{\mathrm{hol}}$ is the SNR for the hologram. Equation (8) is formally equivalent to that derived by Lowenthal *et al.*[20] Assuming detector pixels with statistically independent noise, the noise to image area ratio a'/a in the reconstruction is also the ratio of the number P of independent pixels in the detector to the number of independent samples in the hologram. To reduce the noise, we wish the noise area a' to be as large as possible [Eq. (4)] compared with the image area. The factor $\sqrt{a'/a}$ shows that the SNR in the reconstructed image can be improved at will by averaging each sample of the hologram over a larger number of detector pixels. Equation (8) now gives

$$\mathrm{SNR}_{\mathrm{rec}} = \frac{\sqrt{P/M}}{\sqrt{M}} \mathrm{SNR}_{\mathrm{hol}} = \frac{\sqrt{P}}{M} \mathrm{SNR}_{\mathrm{hol}} \tag{9}$$

III. Discussion

Equation (9) holds for any kind of noise (as long as different pixels have statistically independent noise). It shows that the SNR in the reconstructed image decreases when the image complexity increases.[21] For a given detector (given P) and a given object total flux (given $\mathrm{SNR}_{\mathrm{hol}}$), it is proportional to the inverse of the number M of bright pixels resolved in the object, defined as [Eq. (5)]

$$M = aA = \frac{A}{\bar{o}} \int o(\mathbf{x}) d\mathbf{x}. \tag{10}$$

If the object total flux increases as M, keeping constant the object brightness, one can match the detector size to the object size ($P \propto M$), keeping constant $\mathrm{SNR}_{\mathrm{hol}}$. In this case the SNR decreases with image complexity M only as $1/\sqrt{M}$.

When photon noise is the main source of noise, one has

$$\mathrm{SNR}_{\mathrm{hol}} = \sqrt{N/P}, \tag{11}$$

where N is the total number of photons detected. Putting Eq. (11) into Eq. (9) gives

$$\mathrm{SNR}_{\mathrm{rec}} = \frac{\sqrt{N}}{M}, \tag{12}$$

which is independent of the number of pixels in the detector.

In all cases, the maximum achievable SNR in the reconstructed image depends on the number of detector pixels P and the maximum achievable SNR in the detector, which is determined by its saturation level:

$$(\mathrm{SNR}_{\mathrm{rec}})_{\max} = \frac{\sqrt{P}}{M} (\mathrm{SNR}_{\mathrm{hol}})_{\max} \tag{13}$$

Current charge-coupled device (CCD) chips can store up to 160,000 photoelectrons before saturating, which gives $(\mathrm{SNR}_{\mathrm{hol}})_{\max} = 400$. Hence a commercially available 2048- × 2048-pixel CCD can holographically record a 100 × 100-pixel image with a SNR:

$$\mathrm{SNR}_{\mathrm{rec}} = \frac{2048 \times 400}{10{,}000} = 82. \tag{14}$$

IV. Experimental Setup

To verify the dependence of the SNR on image complexity, measured by the parameter M, we employed a phase-compensated rotational-shear interferometer as described by Roddier *et al.*[23] Incoherent holograms were recorded with a CCD camera[24] using a RCA 512- × 320-pixel detector. However, only 250 × 256 pixels were used for the image reconstruction. The holograms were recorded with broadband white light by means of a chromatic corrector as described in Ref. 15.

In our experiment the color correction is achieved by a system of four afocal triplet lenses, combined with a relay lens, all placed after the interferometer. The relay lens reimages the twin images chromatically dispersed, and the beams expand freely to interfere on the detector. The chromatic dispersion is such that the angular distance between the twin images, as viewed from the detector, is proportional to the wavelength. Since fringe spacing is proportional to both the wavelength and the inverse of this angular distance, it becomes wavelength independent. Indeed by putting in Eq. (1) a magnification factor $k = m\lambda$ proportional to the wavelength λ we have a wavelength-independent illumination:

$$I(\mathbf{u}) = O(0) + \mathrm{Re}O(mR\mathbf{u}). \tag{15}$$

After the chromatic corrector every image point is smeared into a spectrum expanding radially from the optical axis. When interfering on the detector the two beams produced by twin points combine to create white-light fringes. We have counted a few hundred such fringes with the CCD detector. A test using system illumination at a series of discrete wavelengths between 500 and 700 nm showed < 4% error for the desired equally spaced fringes.

An important drawback of incoherent holography is the dc bias produced by the term $O(0)$ in Eq. (15). Another bias term composed of light scattered in the system and dark current of the CCD should be added to this term. To remove these bias terms two holograms were taken per image with the fringe phase flipped 180° between them,[21,25–27] thus flipping the sign of the last term in Eq. (15). Taking the difference between the two (digitized) holograms gives

$$D(\mathbf{u}) = \mathrm{Re}O(mR\mathbf{u}), \tag{16}$$

i.e., a hologram with the bias terms removed. Figure 1 shows an example of hologram obtained with this procedure. It has three advantages:

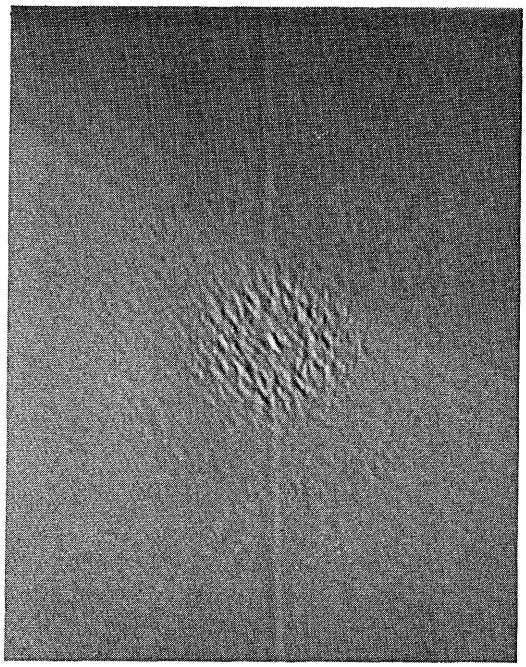

Fig. 1. Incoherent hologram recorded with broadband white light. The dc bias has been removed (background grey level is zero, dark is negative, bright is positive). The object consisted of 40 bright dots.

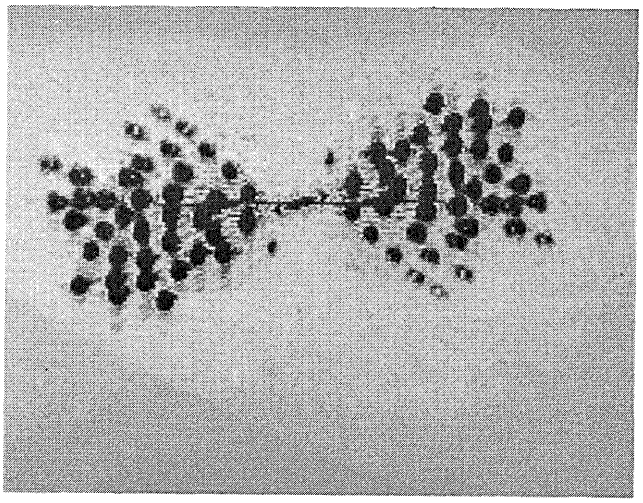

Fig. 2. Reconstructed image obtained by computing the 2-D Fourier transform of the hologram displayed in Fig. 1. The picture is a negative with a reduced dynamic range to better show the noise distribution.

(1) It removes all the bias components including their irrelevant spatial structure.

(2) The noise (contributed mainly by fluctuations in the bias terms) is multiplied by $\sqrt{2}$. But, since the signal is doubled, the SNR increases by a factor of $\sqrt{2}$.

(3) It improves the dynamic range. Although for the CCD readout we still use the same dynamic range, the digital Fourier transform that follows gains from the more limited range of input levels.

We needed an object with a varying and definable degree of complexity. For this purpose, we drilled a large number of round identical holes in a metal plate at random locations. We masked them all with black tape and then unmasked a growing number of holes from the center outward for each hologram. Since the fully exposed mask was very large, the illumination of the holes was slightly different between the center and outer side. The object had, therefore, more than the initially expected two levels of illumination. We estimate the number a'/a of detector pixels per independent area in the hologram to be $\sim$10 for the maximum number of holes (sixty).

V. Experimental Results

The holograms were digitized with a dynamic range of up to 4000 levels. The gain was approximately forty photons per level. The readout noise was low (up to 0.025 of the full range) and, therefore, negligible compared with photon noise. To utilize the full dynamic range, different exposure times were used for different number of holes. The hologram difference shown in Fig. 1 was obtained with forty holes. Hologram differences were Fourier transformed digitally to reconstruct the original object and its twin image. Figure 2 shows the image reconstructed from the hologram of Fig. 1. The noise level in the reconstructed image was measured outside the object extent and found to be uniform all over the reconstruction area as expected.

Since the object had more than two levels of illumination, we defined the object area as the area over which, in each reconstructed point, the signal was above some fraction of its maximum value. The results below were found widely independent of the fraction chosen. This area expressed in number of pixels was taken as our measure of the object complexity M. The SNR in the reconstructed image was obtained by taking the ratio of the signal averaged over the above defined area to the rms noise measured outside the reconstructed object as indicated by Eq. (5).

Assuming pure shot noise, the noise in the hologram was taken as the square root of the average illumination expressed in detected photons per pixels, and the signal was taken as the maximum amplitude of the fringes also expressed in photon units. The SNR in the reconstructed image was then divided by the SNR in the hologram and plotted as a function of M in a log–log scale as shown on Fig. 3. It is clear that for a large object complexity the $1/M$ dependence predicted by Eq. (9) is well observed. However, the factor of proportionality is found to be $\sim$40, well below the factor $\sqrt{P} = 256$ predicted by Eq. (9); i.e., the SNR in the reconstructed image is $\sim$6.4 times lower than the expected value assuming photon noise as the only source of noise in the hologram. The discrepancy is even larger when the image complexity is small.

We believe that these discrepancies can be explained by the imperfections of the optics, such as aberrations, dust, and misalignment of the chromatic corrector. Such errors are highly correlated over different detector pixels and are not included in our modelization. We indeed observed that the point-spread function of the full system is a sharp spike flanked by low-lying

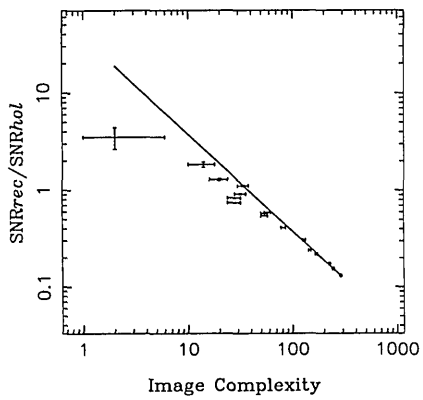

Fig. 3. Ratio of the SNR in the reconstructed image to the SNR in the hologram as a function of the number of bright pixels in the image taken as a measure of its complexity. A minus one slope is shown for comparison with theory.

wide sidelobes. These sidelobes divert power from what we have considered as the reconstructed image (central peaks) and, therefore, produce a lower SNR. When the object consists of closely packed dots the loss of signal power is less severe as observed. The situation is a close analog to that of image reconstruction in radio astronomy where the point spread function is called the dirty beam. Deconvolution techniques such as CLEAN[28] can be used to produce images with an improved SNR.

VI. Summary

We have recorded with a CCD camera holograms obtained with incoherent white-light sources. The SNR in the object reconstruction was compared to theoretical predictions. For complex objects the decrease of the SNR as the inverse of the number of resolved object pixels is well observed. Discrepancies are explained by imperfections in the optics.

References

1. L. Mertz, *Transformations in Optics* (Wiley, New York, 1965).
2. A. Lohmann, "Wavefront Reconstruction for Incoherent Objects," J. Opt. Soc. Am. **55,** 1556 (1965).
3. G. W. Stroke and R. C. Restrick, "Holography with Spatially Incoherent Light," Appl. Phys. Lett. **7,** 229 (1965).
4. G. Cochran, "New Method of Making Fresnel Transforms," J. Opt. Soc. Am. **56,** 1513 (1966).
5. M. V. R. K. Murty and E. C. Hagerott, "Rotational-Shearing Interferometry," Appl. Opt. **5,** 615 (1966).
6. J. B. Breckinridge, "Coherence Interferometer and Astronomical Applications," Appl. Opt. **11,** 2996 (1972).
7. J. B. Breckinridge, "Two-Dimensional White Light Coherence Interferometer," Appl. Opt. **13,** 2760 (1974).
8. J. B. Breckinridge, "A White-Light Amplitude Interferometer with 180-degrees Shear," Opt. Eng. **17,** 156 (1978).
9. F. Roddier and C. Roddier, "Imaging with a Multi-Mirror Telescope," in *Optical Telescopes of the Future, Geneva 1977,* F. Pacini, W. Richter, and R. N. Wilson, Eds. (ESO-CERN, Location, 1978).
10. C. Roddier and F. Roddier, "Imaging with a Coherence Interferometer in Optical Astronomy," in *Formation of Images from Spatial Coherence Functions in Astronomy,* IAU Coll. 49, Van Schooneveld, Ed. (Reidel, Norwell, MA, 1979).
11. F. Roddier, "Rotation-Shearing Interferometry," in *High Angular Resolution Stellar Interferometry,* IAU Coll. 50, J. Davis and W. J. Tango, Eds. (U. Sydney, 1978).
12. K. Itoh and Y. Ohtsuka, "Interferometric Imaging of a Thermally Luminous Two-Dimensional Object," Opt. Commun. **48,** 75 (1983).
13. N. George and S. Wang, "Cosinusoidal Transforms in White Light," Appl Opt. **23,** 787 (1984).
14. S. Wang and N. George, "Fresnel Zone Transforms in Spatially Incoherent Illumination," Appl. Opt. **24,** 842 (1985).
15. C. Roddier, F. Roddier, F. Martin, A. Baranne, and R. Brun, "Twin-Image Holography with Spectrally Broad Light," J. Opt. **11,** 49 (1980).
16. N. George and S. Wang, "Cosinusoidal Transforms in White Light," Appl. Opt. **23,** 787 (1984).
17. S. Wang and N. George, "Fresnel Zone Transforms in Spatially Incoherent White Light," Appl. Opt. **24,** 842 (1985).
18. E. N. Leith and D. K. Angell, "Generalization of Some Incoherent Spatial Filtering Techniques," Appl. Opt. **25,** 499 (1985).
19. P. Connes, "Astronomical Fourier Spectroscopy," Ann. Rev. Astron. Astrophys. **8,** 209 (1970).
20. S. Lowenthal, J. Serres, and H. Arsenault, "Resolution and Film-Grain Noise in Fourier Transform Holograms Recorded with Coherent or Spatially Incoherent Light," Opt. Commun. **1,** 438 (1970).
21. A. Kozma and N. Massey, "Bias Level Reduction of Incoherent Holograms," Appl. Opt. **8,** 393 (1969).
22. A. Papoulis, *Probability, Random Variables and Stochastic Processes* (McGraw-Hill, New York, 1965).
23. F. Roddier, C. Roddier, and J. Demarcq, "A Rotation Shearing Interferometer with Phase-Compensated Roof Prisms," J. Opt. Paris **9,** 145 (1978).
24. Photometrics, Ltd., 2010 N. Forbes Blvd., Suite 103, Tucson, AZ 85745.
25. E. Ribak and E. Leibowitz, "Shearing Stellar Interferometer: 1. Digital Data Analysis Scheme," Appl. Opt. **24,** 3088 (1985).
26. E. Ribak and E. Leibowitz, "Shearing Stellar Interferometer: 2. Optoelectronic Phase Locked System," Appl. Opt. **24,** 3094 (1985).
27. W. T. Rhodes and A. A. Sawchuk, "Incoherent Image Processing," in *Optical Information Processing,* S. H. Lee, Ed. (Springer-Verlag, Berlin, 1981).
28. J. Hogbom, "Aperture Synthesis with a Non-regular Distribution of Interferometer Baselines," Astrophys. J. Suppl. **15,** 417 (1974).

Part of this work was carried out by the Jet Propulsion Laboratory, California Institute of Technology, under contract with the U.S. Army Missile Command at Redstone Arsenal, through the National Aeronautics and Space Administration. Another part was done at NOAO and sponsored by the Strategic Defense Initiative Organization, Office of Innovative Science and Technology, managed by Harry Diamond Laboratories. Erez Ribak is on leave from the Optical Sciences Center, University of Arizona. The National Optical Astronomy Observatories are operated by the Association of Universities for Research in Astronomy, Inc., under contract with the National Science Foundation.